Polymer Chemistry

ROYAL SOCIETY OF CHEMISTRY

COMMUNICATION

View Article Online
View Journal | View Issue

Check for updates

Cite this: *Polym. Chem.*, 2022, **13**, 5458

Received 3rd June 2022,
Accepted 9th September 2022

DOI: 10.1039/d2py00717g

rsc.li/polymers

Published on 15 septembar 2022. Downloaded on 1.2.2026. 23.08.12.

Peptide based folding and function of single polymer chains†

Henrik Kalmer,[a,b] Federica Sbordone[a,b] and Hendrik Frisch *[a,b]

The folding of synthetic polymers into single chain nanoparticles draws inspiration from the folding of polypeptides into the functional macromolecular architectures of proteins. The building blocks of their natural inspiration, amino acids and peptides, are surprisingly underutilised in the design of synthetic folded architectures. Based on N-terminal cysteines, methylmethacrylate derived monomers were designed that are readily copolymerizable with PEGMA and MMA to provide water soluble polymer-peptide conjugates. Upon acidic deprotection of the peptide side chains, disulphide bridges crosslink the parent polymer into a folded architecture. Providing access to functional folded macromolecular architectures, the presented synthetic strategy allows for a facile incorporation of functional amino acid sequences. Embedding of the catalytic triad into pentapeptides containing N-terminal cysteines enabled a one step folding and activation of their catalytic activity as exemplified by hydrolysis of *para*-nitrophenylacetate.

Introduction

Over the last decade, intramolecularly crosslinked synthetic polymers have been established as a distinct class of functional synthetic macromolecular architectures.[1–5] These so called Single Chain Nanoparticles (SCNPs) are investigated for numerous applications spanning sensing,[6] drug delivery[7] and catalysis.[8–11] Their compacted structure has largely been inspired by the reversible folding of polypeptides into functional proteins that is observed in nature.[12,13] The precise architecture, which is obtained upon folding of these sequence-defined biomacromolecules, is encoded into their primary sequence, *i.e.* their monomer sequence. Synthetic efforts have thus also investigated how sequence control can be used to create specifically folded domains within SCNPs and thereby enable control over their 3D-architecture.[14,15]

To introduce the intramolecular crosslinking, a wide range of functional groups has been explored,[16] utilizing for instance photochemistry,[3,17–19] metal-complexation[9,20] or non-covalent interactions.[21,22] Surprisingly, the fundamental monomers of their natural counterparts, *i.e.* amino acids and peptides, have rarely been applied for the folding of synthetic polymer chains.

The enormous potential of peptide derived functional groups to control SCNPs folding has been highlighted by the Knight group. The use of di(phenylalanine) moieties as polymer sidechains enabled the folding of polymers into hydrogen bonded macromolecular architectures.[23] Next to hydrogen-bonds, disulphide bonds are key interactions that stabilise secondary and tertiary structures of proteins. Berda[24] and Thayumanavan[25] implemented disulphide containing crosslinks into SCNPs by either incorporating disulphide containing crosslinkers or disulphide exchange. Elegant work by Lutz[26] attached cysteine–arginine–cysteine (C–R–C) containing linkers to sequence defined polymers in order to obtain bicyclic, 8-shaped polymers.

In solid phase peptide synthesis (SPPS), disulphide formation is often observed upon deprotection of cysteine containing peptides and is usually addressed through cleavage conditions.[27] We report herein a synthetic strategy that exploits disulphide formation upon deprotection of polymer tethered N-terminal cysteines to provide a modular platform to fold single polymer chains in one step (Fig. 1). Seizing the modularity of cysteine terminal monomers, a short catalytically active peptide sequence was introduced into the peptide-based monomer yielding SCNPs with functional folded architectures. The peptide-based sidechain is acting hereby as both the crosslinker and the catalytically active moiety.

[a]*Centre for Materials Science, Queensland University of Technology (QUT), 2 George Street, Brisbane, QLD 4000, Australia*
[b]*School of Chemistry and Physics, Queensland University of Technology (QUT), 2 George Street, Brisbane, QLD 4000, Australia. E-mail: H.Frisch@qut.edu.au*
† Electronic supplementary information (ESI) available. See DOI: https://doi.org/10.1039/d2py00717g

This journal is © The Royal Society of Chemistry 2022

Published on 15 septembar 2022. Downloaded on 1.2.2026. 23.08.12.

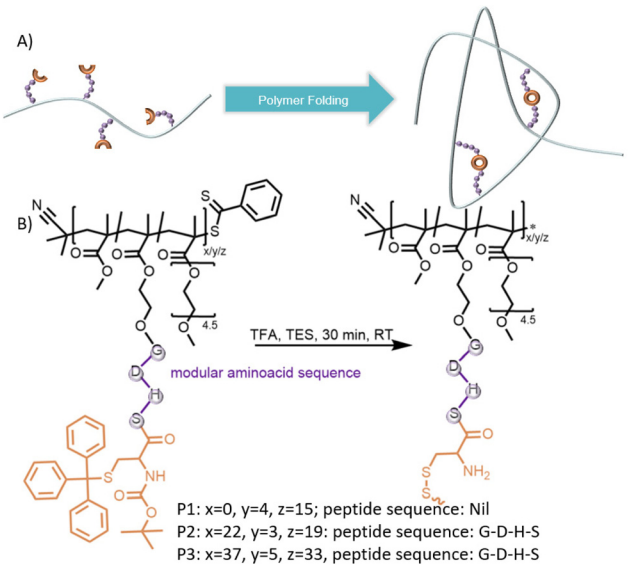

Fig. 1 (A) Schematic representation folding of single polymer chains through cysteine-terminal peptide side chains. (B) Deprotection and concomitant folding of **P1–P3** to **SCNP1–SCNP3**.

Results and discussion

A cysteine-based monomer (**M1**) was synthesized by esterification of protected cysteine (*N*-(*tert*-butoxycarbonyl)-*S*-trityl-L-cysteine) with 2-Hydroxyethylmethacrylate (HEMA, ESI, Chapter 2.1†). Upon reversible addition–fragmentation chain-transfer (RAFT) polymerization with poly(ethylene glycol) methacrylate (PEGMA), a water-soluble polymer **P1** (M_n = 7000 g mol^{-1}, $Đ$ = 1.2) was obtained, containing on average 4 cysteine units. To initiate deprotection of the acid labile protecting groups and concomitant disulphide formation, **P1** was dissolved in a TFA/TES mixture (9 : 1, V : V) at 25 mg mL^{-1} and stirred for 30 minutes at ambient temperature while exposed to air, which has been observed to induce disulphide formation of Cysteinemethylester (Fig. S18†). After precipitation, the folding of the single polymer chains was monitored *via* Size Exclusion Chromatography (SEC, Fig. 2A, top). The obtained **SCNP1** showed a significantly reduced apparent molecular weight from M_p = 7900 (**P1**) to 7000 (**SCNP1**) g mol^{-1} as a result of the decrease in hydrodynamic volume and loss of protecting groups. A high molecular weight shoulder in the SEC trace of **SCNP1** indicates intermolecular crosslinking as a minor side reaction. While the concentration of 25 mg mL^{-1} is high for SCNP folding and facilitates upscaling of the SCNP synthesis,[28] intermolecular crosslinking could not be avoided by lowering the polymer concentration in the folding reaction by more than half to 10 mg mL^{-1} (Fig. S9†). On a molecular level, the successful deprotection of the thiol was monitored *via* ^{1}H nuclear magnetic resonance (NMR) spectroscopy by the significant decrease of aromatic resonances of the trityl-protecting group at δ = 7.5–7.0 ppm and *tert*-butyl resonances at δ = 1.4 ppm (Fig. 2C).

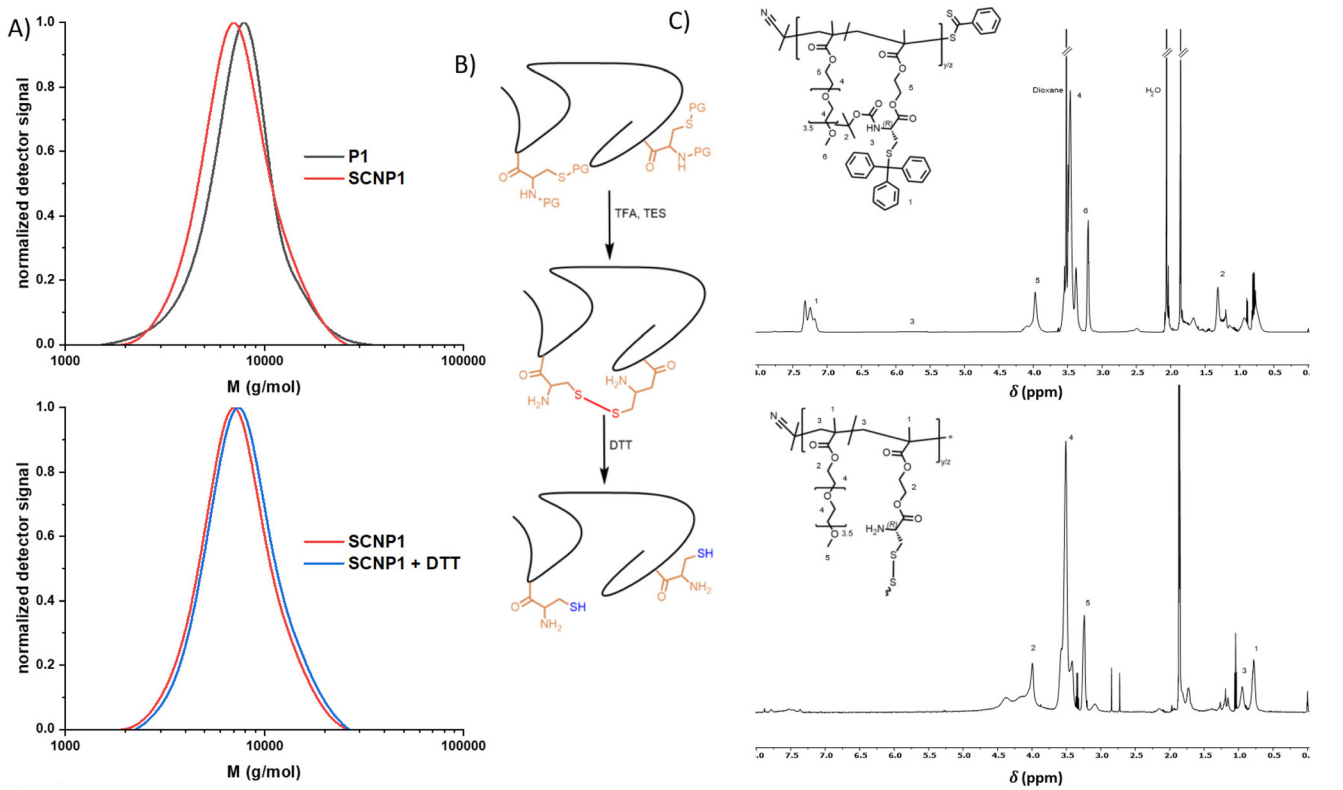

Fig. 2 (A) Overlay of the SEC traces of **P1** and **SCNP1** (top) and **SCNP1** before and after addition of DTT (bottom). (B) Schematic representation of the formation of **SCNP1** *via* disulphide bridges and unfolding of **SCNP1** with DTT. (C) ^{1}H-NMR of P1 and **SCNP1** in acetonitrile-d_3.

Published on 15 septembar 2022. Downloaded on 1.2.2026. 23.08.12.

The residual aromatic resonances indicate a deprotection efficiency of close to 90%. Longer reaction times lead to the full disappearance of aromatic resonances (Fig. S7 and S13†), however, increased intermolecular crosslinking was observed when extending the reaction time too long (Fig. S7 and S14†). Hence, the 30 min deprotection was found preferential to achieve more selective intra chain reactivity.

To confirm that all cysteine moieties have formed intramolecular disulphide crosslinks upon deprotection, an excess of iron(III)chloride hexahydrate, which has been reported to efficiently induce disulphide formation from thiols in SCNPs,[24] was added to the obtained **SCNP1**. However, no shift towards lower apparent molecular weights was observed *via* SEC (ESI, Chapter 2.6†). In contrast, a shoulder towards higher molecular weights appeared, indicating intermolecular crosslinking of the remaining cysteine moieties. DTT, a common disulphide bridge reducing agent in proteins, was added after the SCNP-formation to unfold the polymer chain (SEC, Fig. 2A, bottom). The unfolding lead to a shift in the SEC trace due to the larger hydrodynamic volume of the unfolded chain, to an apparent molecular weight of M_p = 7300 g mol^{-1}, a behaviour that is in agreement with previously reported disulphide based SCNP unfolding.[24,25]

To investigate the modularity of the developed synthetic approach, a short tetrapeptide (G–D–H–S) was juxtaposed to the terminal cysteine. The D–H–S sequence, often labelled catalytic triad, is found in the active site of a wide range of enzymes able to catalyse for example ester hydrolysis.[29,30] The propensity of D–H–S and derived peptide sequences to cleave esters as both individual peptides[31] and peptide-polymer conjugates[32,33] has shown great potential for the design of artificial enzyme mimetics.

The C-terminus of otherwise fully protected peptide sequence (G–D–H–S–C) obtained *via* SPPS was esterified with HEMA, yielding monomer **M2**. After RAFT mediated copolymerization with methyl methacrylate (MMA) and PEGMA, water-soluble polymer **P2** was obtained (M_n = 11 600 g mol^{-1}, $Đ$ = 1.2), containing on average 3 sidechain tethered peptide units. **P2** was dissolved in a TFA/TES mixture (8 : 2, V : V) at 7.5 mg mL^{-1} and stirred for 30 minutes at ambient temperature while exposed to air to obtain **SCNP2** after precipitation. The deprotection and folding was monitored *via* SEC showing a reduced apparent molecular weight from M_p = 12 400 (**P2**) to 11 200 (**SCNP2**) g mol^{-1} due to the polymer compaction (Fig. 3A and B, top). Intermolecular crosslinking, however, could also for **SCNP2** not be avoided, hence the SEC traces show a slight high molecular weight shoulder. Similarly to **SCNP1**, **SCNP2** reduction with DTT resulted in a shift towards larger apparent molecular weights (M_p = 12 100 g mol^{-1}, Fig. 3A and B, bottom). The deprotection was monitored *via*

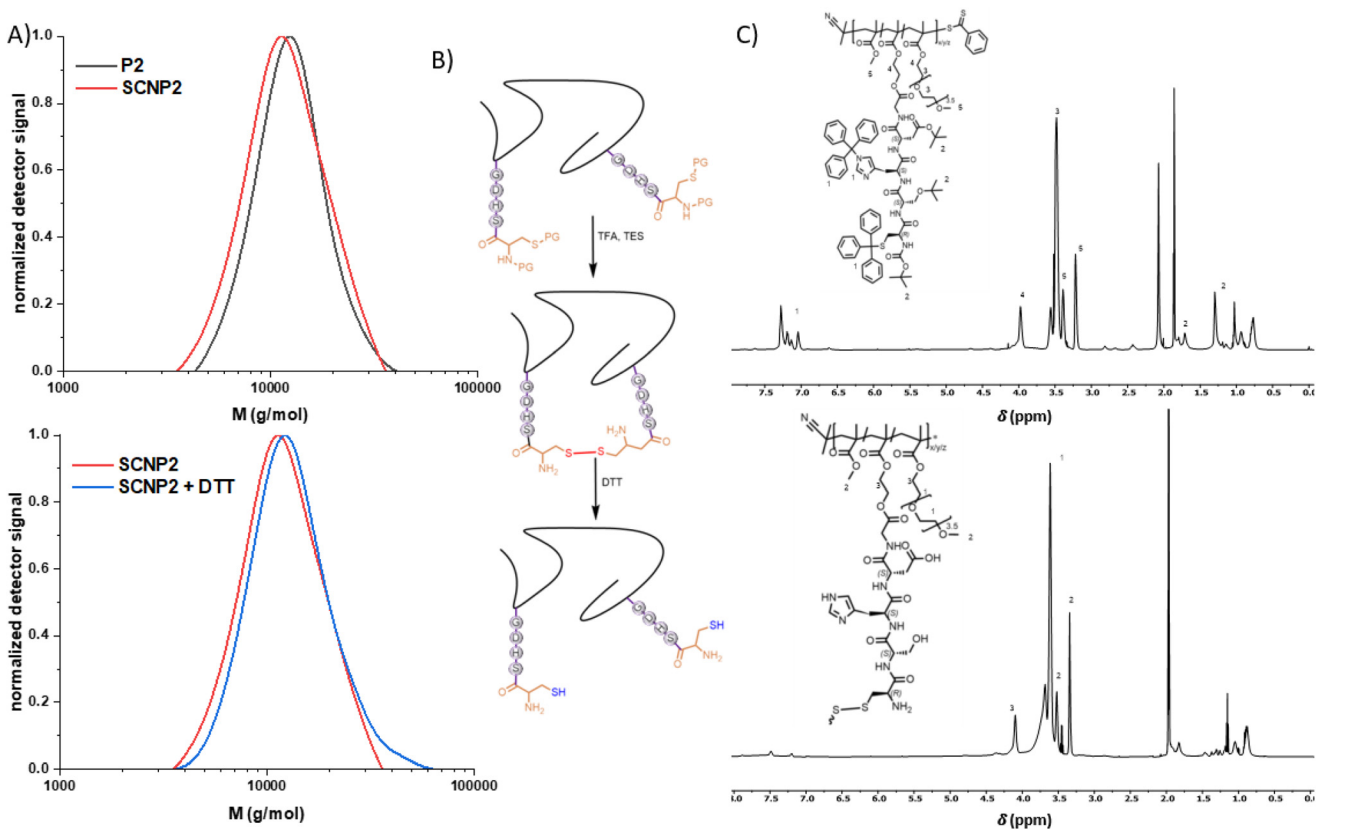

Fig. 3 (A) Overlay of the SEC traces of **P2** and **SCNP2** (top) and **SCNP2** before and after addition of DTT (bottom). (B) Schematic representation of the formation of **SCNP2** *via* disulphide bridges and unfolding of **SCNP2** with DTT. (C) ^{1}H-NMR of **P2** and **SCNP2** in acetonitrile-d_3.

 This journal is © The Royal Society of Chemistry 2022

Published on 15 septembar 2022. Downloaded on 1.2.2026. 23.08.12.

^{1}H-NMR showing the loss of resonances of the trityl (δ = 7.4–7.2 ppm) and *tert*-butyl (δ = 1.4 and 1.1 ppm) protecting groups (Fig. 3C). To investigate the effect of the number of catalytically active peptide pendants per chain on the desired catalytic performance, a third polymer **P3** was synthesized (M_p = 21 200 g mol^{-1}, ESI†) using the same procedure as described for **P2**. The deprotection lead to a shift to lower apparent molecular weights (M_p = 20 000 g mol^{-1}). Monitoring of monomer incorporation *via* 1H-NMR indicated a random copolymer of PEGMA and M2 with a slight gradient of MMA (Table S1†).

Finally, the propensity of **SCNP1–SCNP3** towards the hydrolysis of esters was investigated. *para*-Nitrophenyl acetate (*p*-NPA) was dissolved in a phosphate buffered aqueous solution (pH = 7). The hydrolysis of *p*-NPA leads to the formation of *para*-nitrophenol, which absorbs visible light at λ = 405 nm. The absorption was recorded for 40 minutes *via* UV/VIS spectroscopy. Addition of **SCNP2** lead to significantly faster linear increase in absorbance compared to the auto hydrolysis of *p*-NPA under the same conditions (Fig. 4). Since the concentration of the *p*-nitrophenol is proportional to the absorption at 405 nm, the steeper slope indicates a faster reaction rate due to the catalytic activity of **SCNP2**. In the presence of **SCNP2** the hydrolysis is faster compared to the uncatalysed reaction. To demonstrate that the observed ester hydrolysis activity is a function of the amino acid sequence of **SCNP2** and not the terminal cysteines linker, the same experiment was carried out using **SCNP1**, showing no impact on the hydrolysis rate. The origin of the catalytic activity of **SCNP2** can therefore be directly assigned to the peptide sequence in its sidechains. Remarkably, the hydrolysis rate of **SCNP2** was significantly faster compared to non-polymer tethered GDHSC peptide, which only showed very little catalytic activity at the same overall concentration of peptide. When the degradation rate of *p*-NPA in presence of the unprotected peptide sequence was investigated at different concentrations of GDHSC, the expected concentration dependence was, however, observed (Fig. S19†).

Comparing **SCNP2** to **SCNP3** of a higher molecular weight and greater number of peptide moieties per chain, a considerably higher hydrolysis activity was observed for **SCNP3** indicating a significant effect of polymer confinement on the hydrolysis activity of GDHSC. The addition of DTT to **SCNP3**, resulting in SCNP unfolding, lead to a decrease of the catalytic activity by close to 50%. Adding DTT to a reference experiment, in contrast, did not affect the degradation rate. Hence, the folded SCNP architecture appears to impact catalytic activity.

Noting that catalysis of DHS based enzymes occurs from the precise 3D arrangement of amino acids, which are usually not adjacent in the primary structure, these results raise questions for future investigations about how discrete SCNP architectures increase catalytic activity. Underlying effects could include changes in the conformation of individual peptide strands, closer proximities between peptides strands that enable catalysis involving multiple peptides as well as changes in local polarity within the polymer coil.

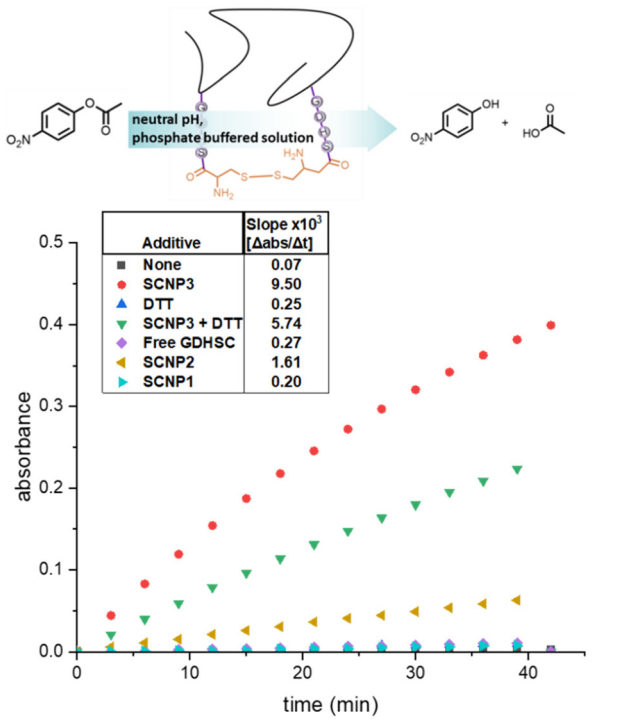

Fig. 4 Schematic degradation of *para*-nitrophenylacetate to *para*-nitrophenol and acetic acid, catalysed by **SCNP2** (top). Change of absorption at 405 nm over time (bottom) due to the hydrolysis of *p*-NPA for **SCNP1–SCNP3**, **SCNP3** + DTT, and free GDHSC.

Conclusions

We herein reported a modular synthetic strategy to fold single polymer chains upon deprotection of pendent N-terminal cysteines (**P1**, **P2**, **P3**). One step deprotection and folding of single polymer chains *via* disulphide bridges was achieved at concentrations of up to 25 mg mL^{-1} (**SCNP1**). Demonstrating the modularity of the synthetic strategy, a short peptide sequence of G–D–H–S was juxtaposed to the N-terminal cysteine (**P2**). Deprotection of the amino acid sequence and folding of the polymer chain into **SCNP2** was performed in one step, yielding a catalytically active D–H–S triad. The catalytic activity of **SCNP2** was demonstrated through the hydrolysis of *p*-NPA, accelerating hydrolysis significantly compared to non-polymer tethered peptide of the same concentration. Increasing the number of pendent peptides per polymer chain (**SCNP3**) further increased the hydrolysis rate, whereas the addition of DTT induced unfolding and a substantial decrease in hydrolysis rate. The pendent peptide moieties thus induce folding and enable function of single polymer chains.

In addition to the design of enzyme mimetic systems, the reported strategy may provide access to synthetic polymers with defined intramolecular architectures through the incorporation structurally encoded peptide sequences such as α-helices.

Published on 15 septembar 2022. Downloaded on 1.2.2026. 23.08.12.

Conflicts of interest

There are no conflicts to declare.

Acknowledgements

H. F. acknowledges the Australian Research Council for a Discovery Early Career Researcher Award (DECRA) as well as continued support from QUT through the Centre for Materials Science and School of Chemistry and Physics. H. F. acknowledges Prof. Christopher Barner-Kowollik (QUT) for sponsoring and mentorship of his research activities in the context of his ARC Laureate Fellowship. H. K. acknowledges a scholarship from the School of Chemistry and Physics. The authors are grateful to Dr Bryan Tuten (QUT), Dr Aaron Micallef (QUT) and Aidan Izuagbe (QUT) for insightful discussions on disulphide formation within SCNPs.

References

1 H. Frisch, B. T. Tuten and C. Barner-Kowollik, *Isr. J. Chem.*, 2020, **60**, 86–99.
2 M. A. M. Alqarni, C. Waldron, G. Yilmaz and C. R. Becer, *Macromol. Rapid Commun.*, 2021, **42**, 2100035.
3 O. Galant, H. B. Donmez, C. Barner-Kowollik and C. E. Diesendruck, *Angew. Chem., Int. Ed.*, 2021, **60**, 2042–2046.
4 R. Chen, S. J. Benware, S. D. Cawthern, J. P. Cole, J. J. Lessard, I. M. Crawford-Eng, R. Saxena and E. B. Berda, *Eur. Polym. J.*, 2019, **112**, 206–213.
5 J. Rubio-Cervilla, E. onzález and J. A. Pomposo, in *Single-Chain Polym. Nanoparticles*, 2017, pp. 341–388.
6 L. Deng, L. Albertazzi and A. R. A. Palmans, *Biomacromolecules*, 2022, **23**, 326–338.
7 A. P. P. Kröger and J. M. J. Paulusse, *J. Controlled Release*, 2018, **286**, 326–347.
8 A. Sanchez-Sanchez, A. Arbe, J. Colmenero and J. A. Pomposo, *ACS Macro Lett.*, 2014, **3**, 439–443.
9 N. D. Knöfel, H. Rothfuss, J. Willenbacher, C. Barner-Kowollik and P. W. Roesky, *Angew. Chem., Int. Ed.*, 2017, **56**, 4950–4954.
10 Z. Hu and H. Pu, *Eur. Polym. J.*, 2021, **143**, 110194.
11 Y. Liu, P. Turunen, B. F. M. de Waal, K. G. Blank, A. E. Rowan, A. R. A. Palmans and E. W. Meijer, *Mol. Syst. Des. Eng.*, 2018, **3**, 609–618.
12 C. M. Dobson, *Nature*, 2003, **426**, 884–890.
13 M. H. Barbee, Z. M. Wright, B. P. Allen, H. F. Taylor, E. F. Patteson and A. S. Knight, *Macromolecules*, 2021, **54**, 3585–3612.
14 J. Zhang, G. Gody, M. Hartlieb, S. Catrouillet, J. Moffat and S. Perrier, *Macromolecules*, 2016, **49**, 8933–8942.
15 J. Zhang, J. Tanaka, P. Gurnani, P. Wilson, M. Hartlieb and S. Perrier, *Polym. Chem.*, 2017, **8**, 4079–4087.
16 S. Mavila, O. Eivgi, I. Berkovich and N. G. Lemcoff, *Chem. Rev.*, 2016, **116**, 878–961.
17 H. Frisch, D. Kodura, F. R. Bloesser, L. Michalek and C. Barner-Kowollik, *Macromol. Rapid Commun.*, 2019, 1900414.
18 D. Kodura, H. A. Houck, F. R. Bloesser, A. S. Goldmann, F. E. Du Prez, H. Frisch and C. Barner-Kowollik, *Chem. Sci.*, 2021, **12**, 1302–1310.
19 P. G. Frank, B. T. Tuten, A. Prasher, D. Chao and E. B. Berda, *Macromol. Rapid Commun.*, 2014, **35**, 249–253.
20 A. Levy, R. Feinstein and C. E. Diesendruck, *J. Am. Chem. Soc.*, 2019, **141**, 7256–7260.
21 P. J. M. Stals, M. A. J. Gillissen, T. F. E. Paffen, T. F. A. de Greef, P. Lindner, E. W. Meijer, A. R. A. Palmans and I. K. Voets, *Macromolecules*, 2014, **47**, 2947–2954.
22 T. Mes, R. van der Weegen, A. R. A. Palmans and E. W. Meijer, *Angew. Chem., Int. Ed.*, 2011, **50**, 5085–5089.
23 J. L. Warren, P. A. Dykeman-Bermingham and A. S. Knight, *J. Am. Chem. Soc.*, 2021, **143**, 13228–13234.
24 B. Tuten, D. Chao, C. Lyon and E. B. Berda, *Polym. Chem.*, 2012, **3**, 3068–3071.
25 C. Song, L. Li, L. Dai and S. Thayumanavan, *Polym. Chem.*, 2015, **6**, 4828–4834.
26 O. Shishkan, M. Zamfir, M. A. Gauthier, H. G. Börner and J. F. Lutz, *Chem. Commun.*, 2014, **50**, 1570–1572.
27 P. R. Singh, M. Rajopadhye, S. L. Clark and N. E. Williams, *Tetrahedron Lett.*, 1996, **37**, 4117–4120.
28 A. M. Hanlon, R. Chen, K. J. Rodriguez, C. Willis, J. G. Dickinson, M. Cashman and E. B. Berda, *Macromolecules*, 2017, **50**, 2996–3003.
29 E. Di Cera, *IUBMB Life*, 2009, **61**, 510–515.
30 L. Polgár, *Cell. Mol. Life Sci.*, 2005, **62**, 2161–2172.
31 Y. Li, Y. Zhao, S. Hatfield, R. Wan, Q. Zhu, X. Li, M. McMills, Y. Ma, J. Li, K. L. Brown, C. He, F. Liu and X. Chen, *Bioorg. Med. Chem.*, 2000, **8**, 2675–2680.
32 M. D. Nothling, A. Ganesan, K. Condic-Jurkic, E. Pressly, A. Davalos, M. R. Gotrik, Z. Xiao, E. Khoshdel, C. J. Hawker, M. L. O'Mara, M. L. Coote and L. A. Connal, *Chem*, 2017, **2**, 732–745.
33 C. Douat-Casassus, T. Darbre and J.-L. Reymond, *J. Am. Chem. Soc.*, 2004, **126**, 7817–7826.

 This journal is © The Royal Society of Chemistry 2022